

# **Eng, S.C.W., "Improvement on the Design and Simulation of an Electromagnetic Actuator for Active Vibration Control", Undergraduate Thesis, University of Western Australia.**

[...]

## **5 MATERIAL SELECTIONS**

### **5.1 Materials**

The material used in constructing the electromagnetic actuator is the most important aspect of the whole design due to the fact that the permeability of a metal greatly affects the force output and performance. Traditional electromagnetic actuators have always been made by steel and laminated steel; mostly mild steel due to their low price and high machinability. However, further research showed that the materials required to manufacture an electromagnetic actuator are not mentioned and if yes, briefly, due to the unknown and non-linear outcome it poses. In this dissertation, only ferromagnetic metals and alloys will be subjected to discussion. Mild Steel, Iron and Cast Iron were subjected to continuous electromagnetic simulation and their effects on the force output will be presented. Mild Steel and Cast Iron are both widely available in any workshops with high machinability. Choosing one of them as the manufacturing material requires extensive testing and will be costly in real life.

#### **5.1.1 Iron**

The purer the iron, the higher the relative permeability is. However, pure iron is very ductile and malleable in nature and addition of impurities such as carbon and chromium are crucial to transform it into strong alloys like mild steel and cast iron. Although it is not realistic to simulate iron as a material intended to be used for manufacturing, its relative permeability (5000) is close to that of mild steel. Iron, mild steel and cast iron will be subjected to the same settings and inputs during simulation to find out the difference caused by varying carbon contents in ferromagnetic alloys.

#### **5.1.2 Mild Steel**

Mild steel are also known as medium-carbon steels. They have carbon concentration in between 0.25 and 0.60 wt% (Callister 1994, p. 354) and are widely used in tempered condition with microstructures of tempered martensite. The strength and ductility of the alloy

can be altered by adding chromium, nickel, and molybdenum. Applications of mild steel include gears, crankshafts, railway wheels and high strength structural components in need of a combination of wear resistance, toughness and high strength. The relative permeability of mild steel is 2000.

### **5.1.3 Cast Iron**

Cast Iron has carbon contents typically above 2.1 wt%. In the engineering field, C contents between 3.0 and 4.5 wt% are widely used (Callister 1994, p.357). They are brittle because of the high carbon contents, making casting the most appropriate technique for fabrication. For most cast irons, carbon exists as graphite and both microstructure and mechanical aspects of the alloy depends on the content and treatment it will be subjected to. Applications of cast iron are cylinder blocks, gearbox cases, construction of buildings, etc due to their excellent resistant to destruction and corrosion. The relative permeability of cast iron is 600.

### **5.2 Simulation Software**

The software used to simulate the actuator under different settings is ElectroMagneticWorks (EMW) and is a certified gold add-in by SolidWorks, a well-known 3D modelling software. It computes important parameters such as force, torque, magnetic flux density, magnetic field, electric field, electric flux, current flow, eddy current, inductance, capacitance, resistances, flux linkage, and power loss. A contract was signed beforehand to use the software for educational purposes.

### **5.3 Testing and Procedures**

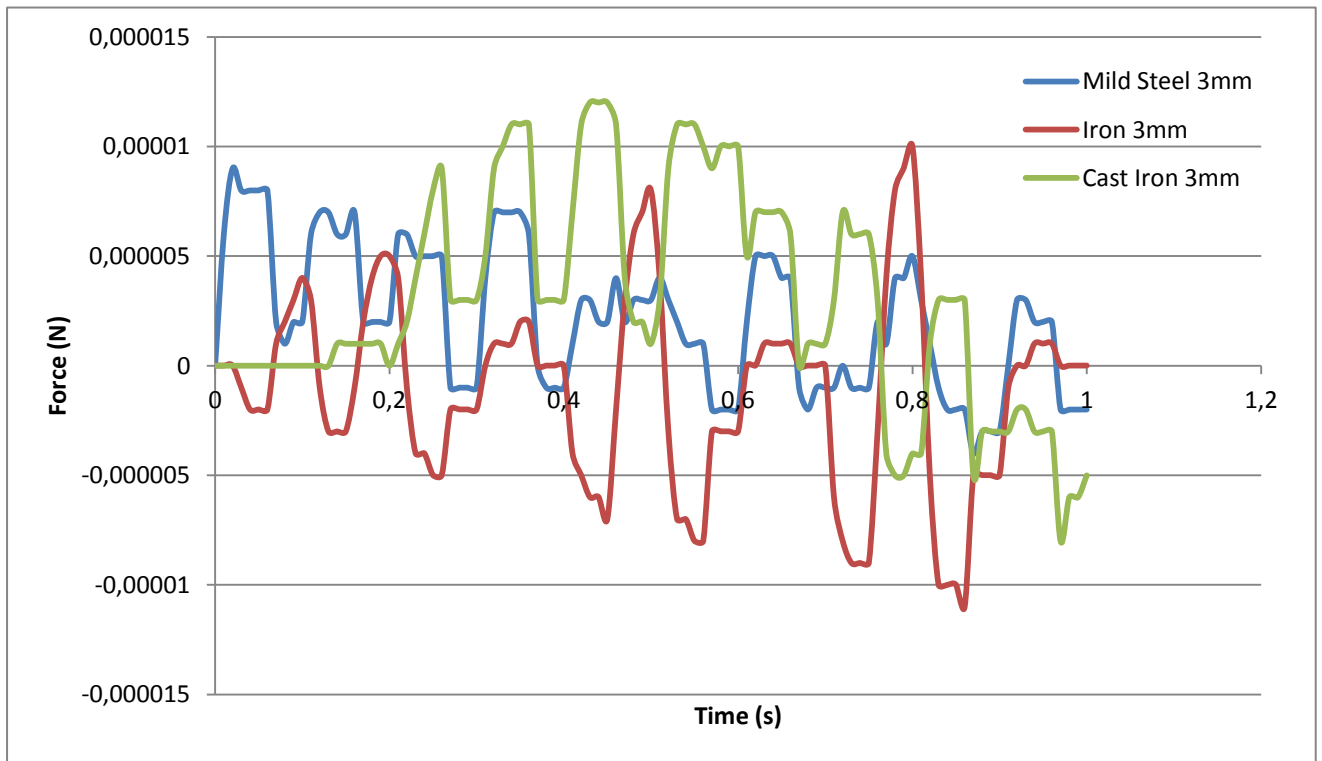
At first, materials are assigned to each part of the actuator as shown in Figure 4-8. The direction of the current in each coil was set in a direction so that its direction of magnetic field will be aimed at the surface of the thrust disc. The PMs on the thrust disc was assigned as Grade 1 ceramic ferrite magnets. Acrylic tube and brass bush were assigned as air to neglect their effects (material not available) on the simulation and other parts set to each respective metal. Each set of coils were given 180 turns of wire as calculated and current input was set as a pulse current source with a 0.05 s delay between two coils. The electromagnetic actuator was meshed and studies ran for air gaps 3 mm, 2 mm, 1 mm, and 0.5 mm, repeating for each material and had an average running time of 1.5 hours per study.

Maximum Current, I,max (A)	Minimum Current, I,max (A)	Rise Time, TR (s)	Fall Time, TF (s)	Pulse Width, PW (s)	Pulse Period, PER (s)
3	0	0.0125	0.0125	0.05	0.1

**Table 5-1:** Input settings for Pulse Current Source in EMW

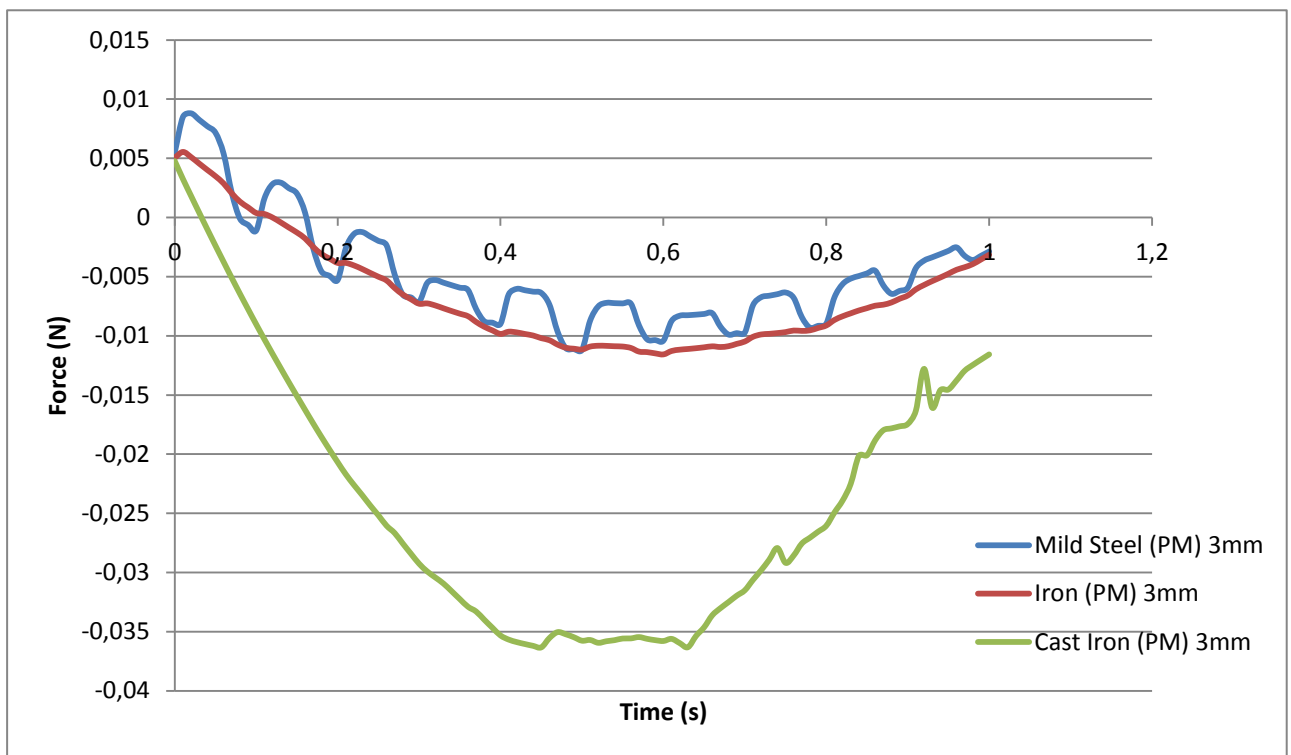
## 5.4 AIR GAPS

### 5.4.1 Air Gap of 3 mm



**Graph 5-1:** Force (N) vs Time (s) with at an air gap of 3 mm

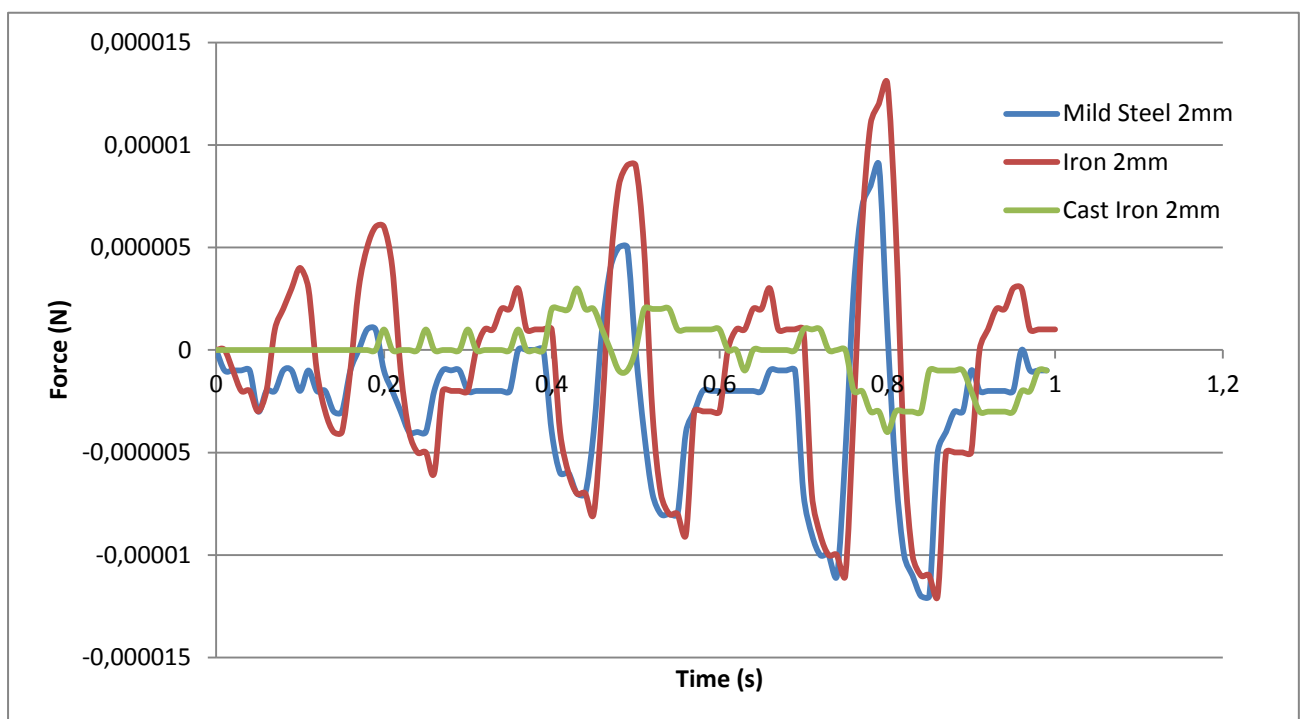
**Observation:** Without PM, Mild Steel fluctuated with an irregular pattern in the positive y-axis, hard to predict and can be seen shifting its equilibrium downwards. Iron is relatively stable and displays close sinusoidal pattern with a slight increase in amplitude after each successive period. Cast Iron showed signs of change after 0.1 seconds, increasing its predictable path above the y-axis and gradually decreasing its amplitude and shifting its equilibrium to the negative y-axis when approaching 1 second.



**Graph 5-2:** Force (N) vs Time (s) with PM at an air gap of 3 mm

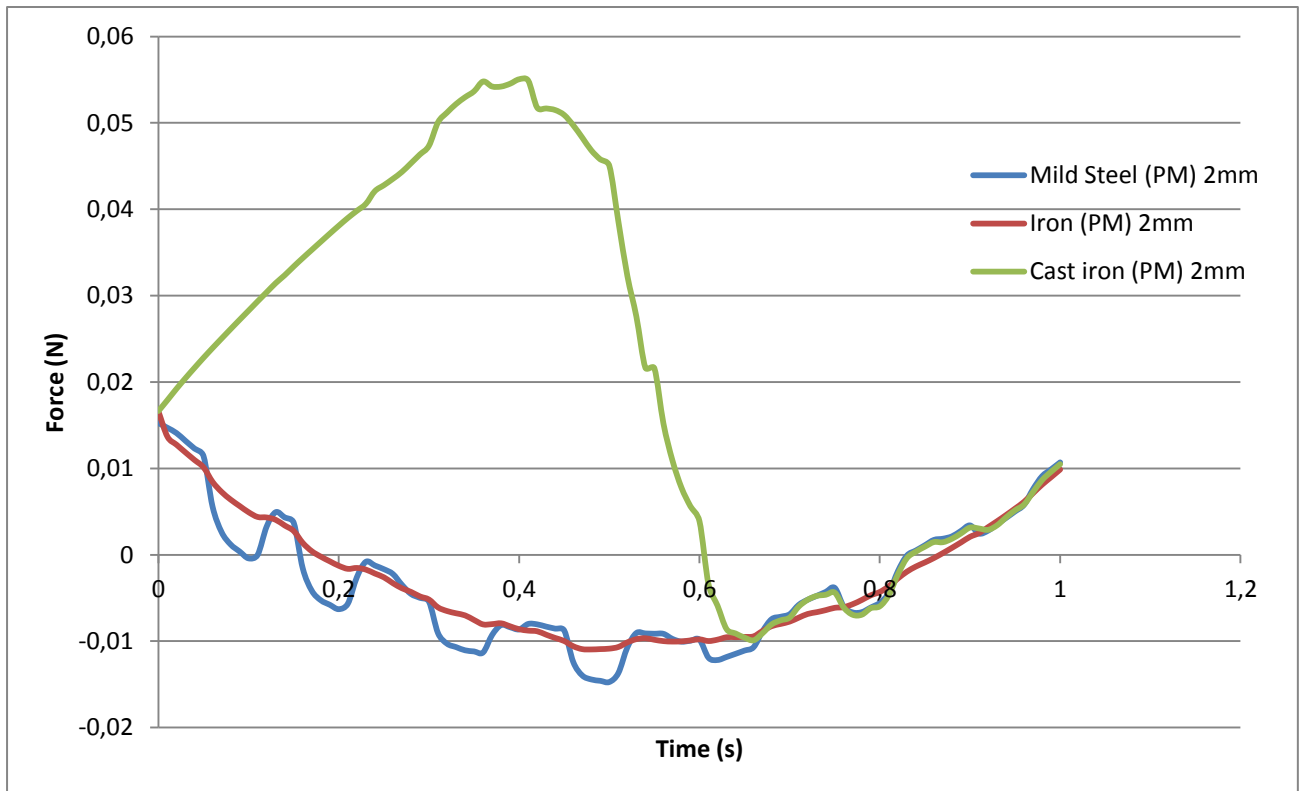
**Observation:** With the presence of a permanent magnet, Mild Steel started at 0.005 N at 0 seconds alongside with Iron and Cast Iron. Mild Steel had a near sinusoidal pattern with Iron following its path, showing no major change towards the alternating magnetic field. On the other hand, Cast Iron showed a larger magnitude in the negative y-axis with little sensitivity to the change of magnetic fields before 0.4 seconds.

### 5.4.2 Air Gap of 2 mm



**Graph 5-3:** Force (N) vs Time (s) at an air gap of 2 mm

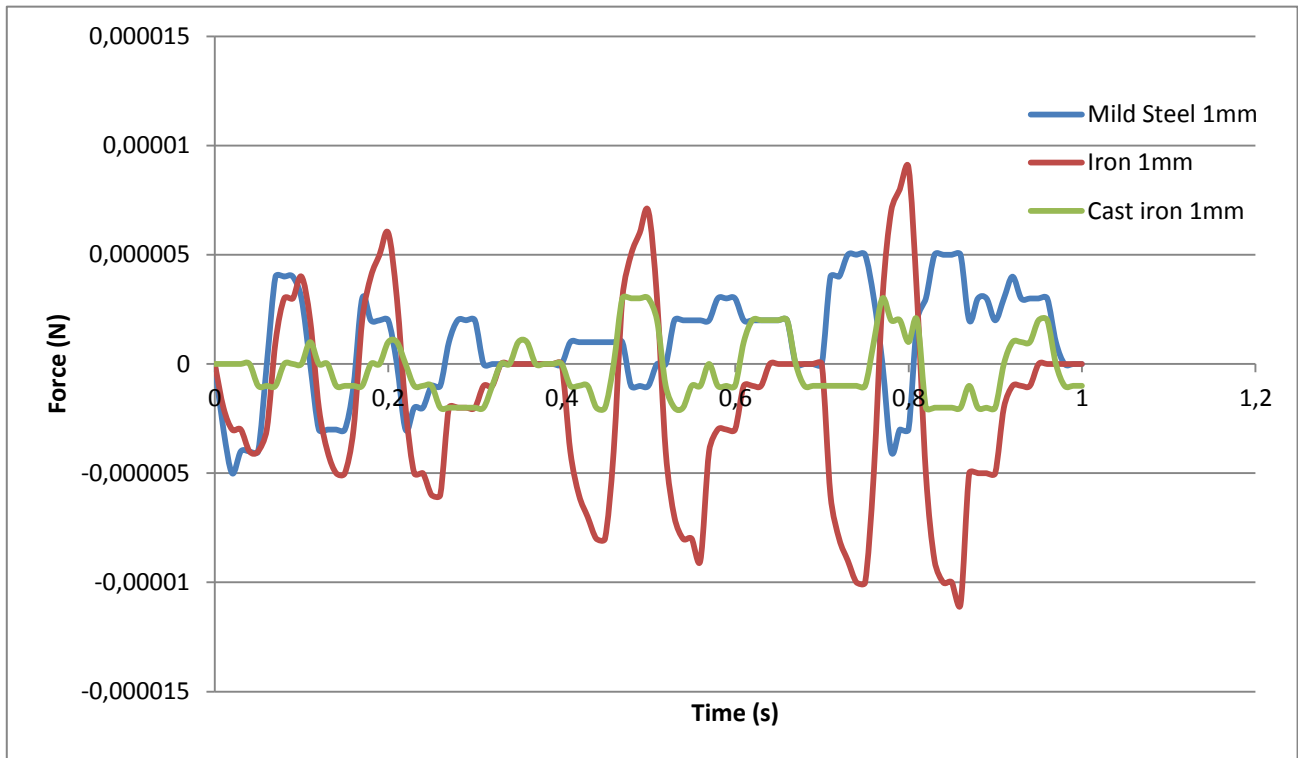
**Observation:** At an air gap of 2 mm, Mild Steel started off in the negative y-direction with minor oscillations and showed near sinusoidal pattern with an increasing rate after each successive period. Iron started off just as Mild Steel but had larger amplitude at 0.1 s with successive oscillations being slightly larger than Mild Steel. Cast Iron only showed changes at 0.2 s with minor amplitude and irregular oscillations towards the end of 1 s.



**Graph 5-4:** Force (N) vs Time (s) with PM at an air gap of 2 mm

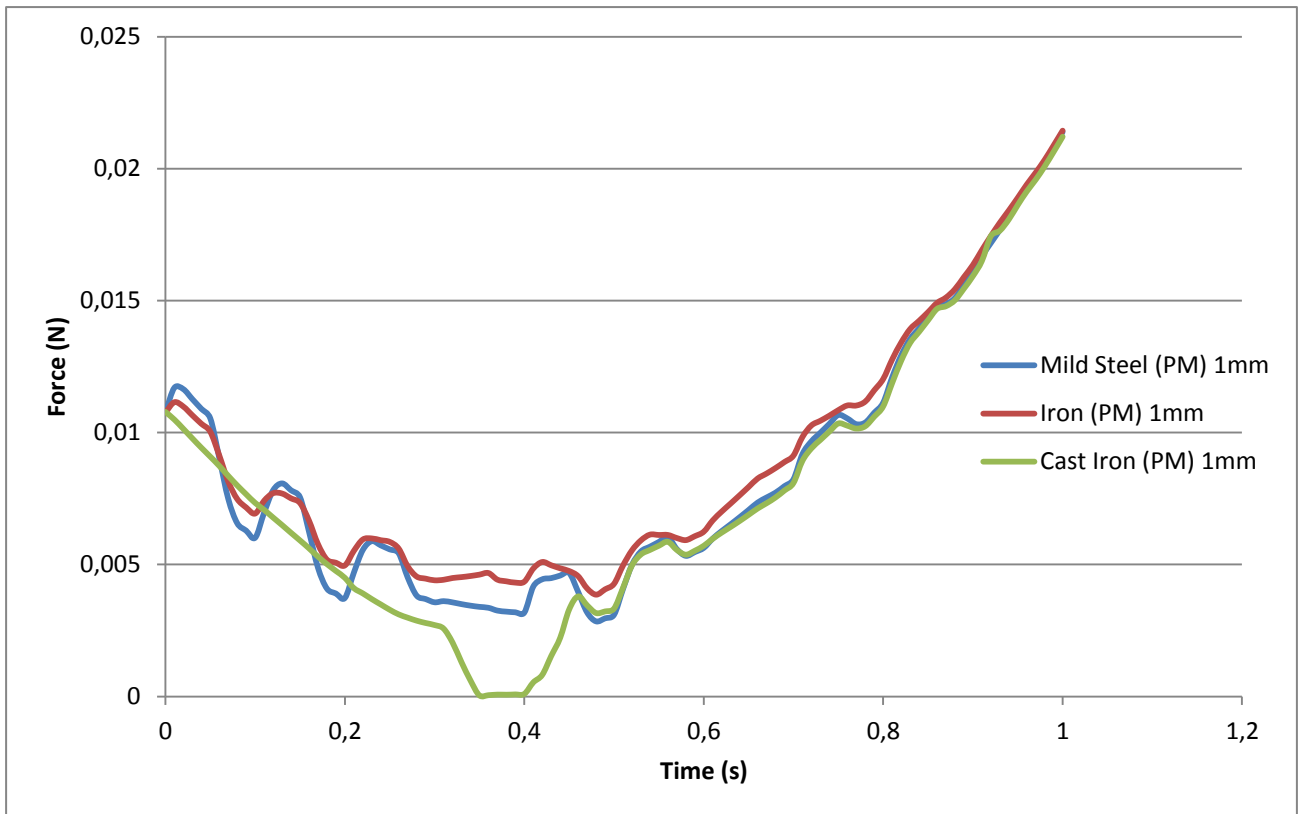
**Observation:** With a magnet, all three alloys started at a force of 0.017 N at 0 s. Mild Steel showed its sensitivity towards the changing magnetic field with a decrease in oscillation amplitude towards the end. Iron followed Mild Steel's path without any obvious oscillation pattern. Cast iron surged in the positive y-direction and had a peak magnitude of 0.055 N at 0.42 s and decreases till it joined Mild Steel's oscillating curve.

### 5.4.3 Air Gap of 1 mm



**Graph 5-5:** Force (N) vs Time (s) at an air gap of 1mm

**Observation:** Mild Steel started its oscillation in the negative y-direction and shows unpredictable and often stagnant plots in between successive oscillation. Iron started off like Mild Steel but has a more defined oscillation with increasing amplitude after each successive oscillation. Cast Iron showed low magnitude plots with near sinusoidal pattern and resembles Mild Steel's plot with an inverse phase.

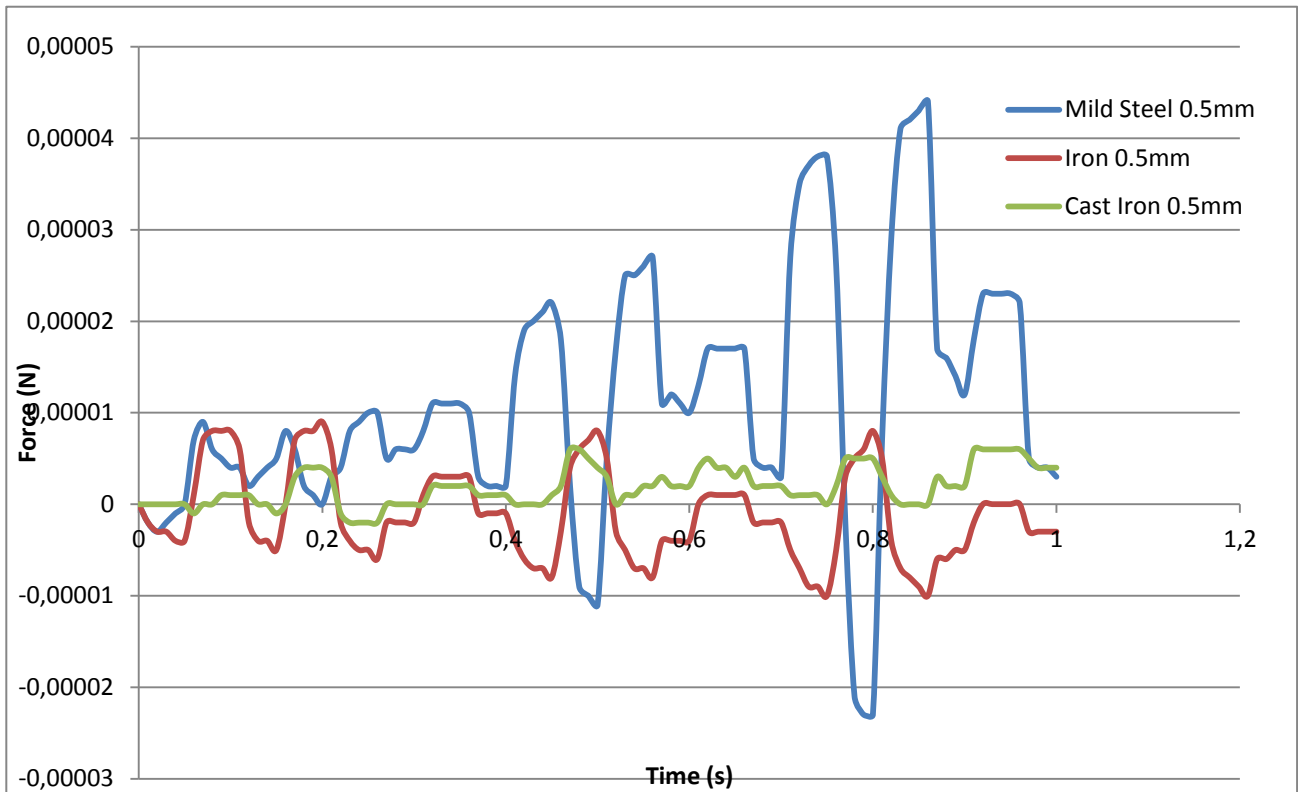


**Graph 5-6:** Force (N) vs Time (s) with PM at an air gap of 1 mm

**Observation:** With a magnet, the plot started at 0.012 N for all three metals. Mild Steel and Iron showed similar plots with Iron lacking in magnitude. Cast Iron didn't show any changes and drops to 0 N in between 0.35 - 0.4 s and joined Mild Steel and Iron's plot at approximately 0.5 s.

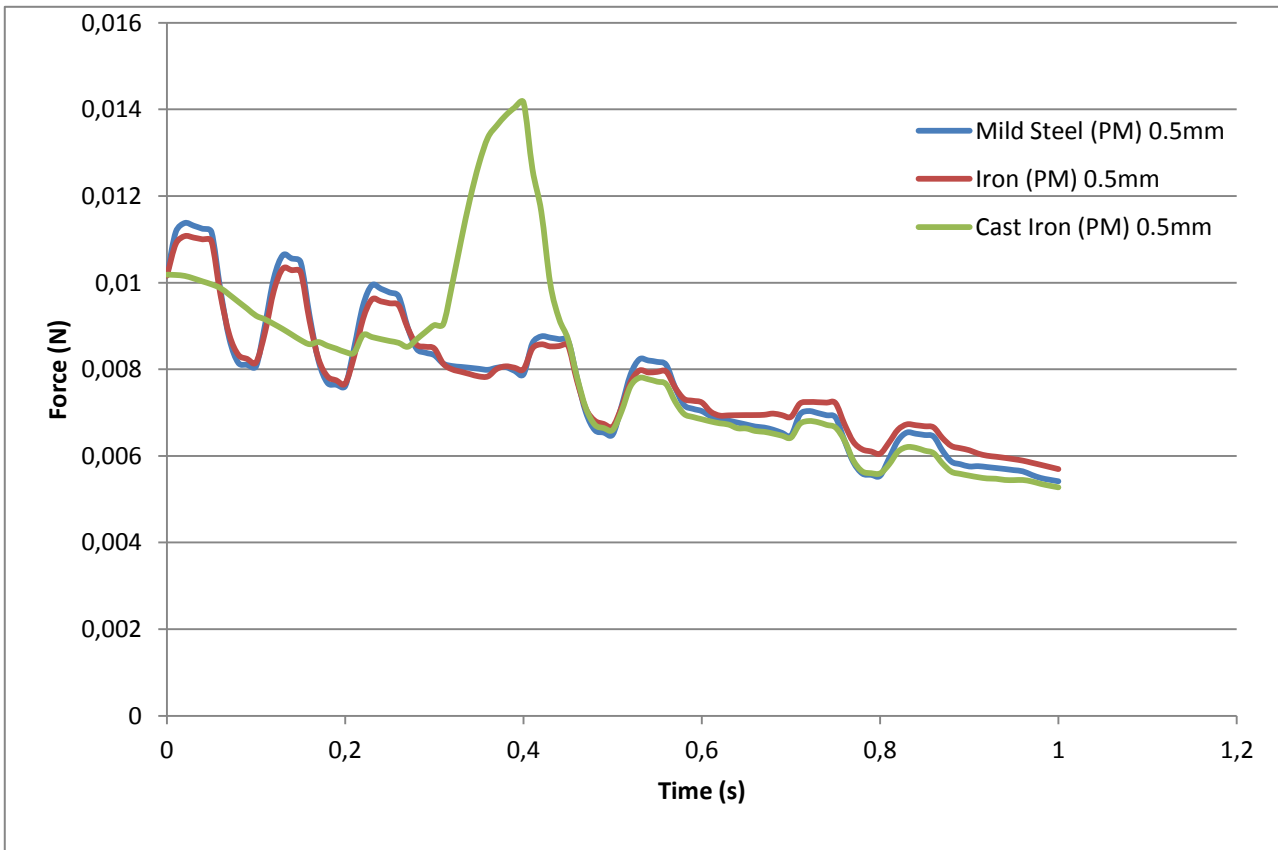


#### 5.4.4 Air Gap of 0.5 mm



**Graph 5-7:** Force (N) vs Time (s) at an air gap of 0.5mm

**Observation:** Mild Steel mainly oscillates in the positive y-axis and increases its amplitude significantly after 0.4 s and decreases at the very end. Iron oscillates and showed near sinusoidal pattern with predictable and stable plots. On the other hand, Cast Iron showed minor changes to the changing magnetic field but its amplitude is greatly insignificant if compared to Mild Steel and Iron.

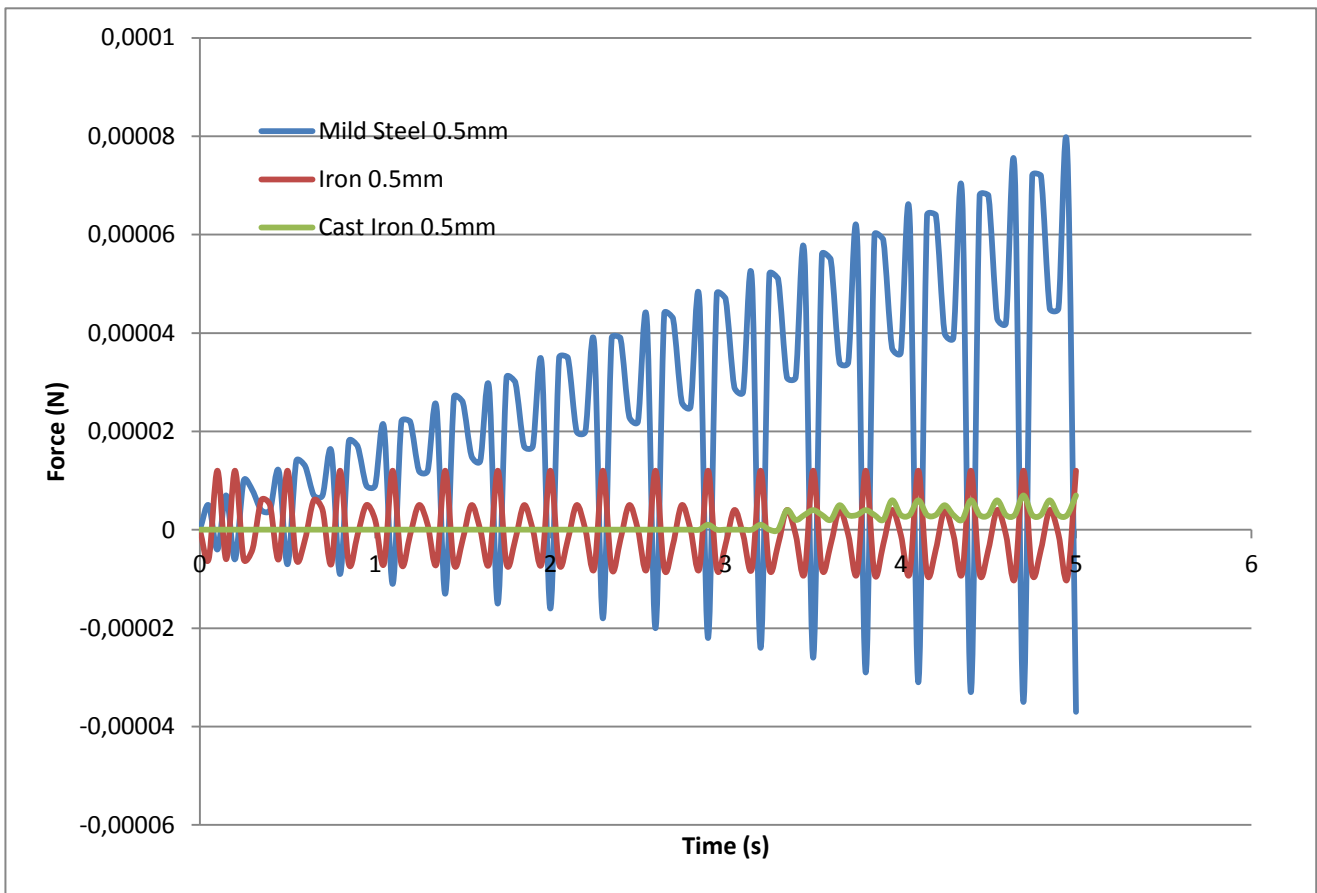


**Graph 5-8:** Force (N) vs Time (s) with PM with an air gap of 0.5mm

**Observation:** With the presence of a PM, the plot started at 0.01 N, Mild Steel and Iron showed near sinusoidal pattern and at the same time shifting their equilibrium to the negative y-direction. Cast Iron had little oscillations and showed a peak magnitude at 0.4 s. It then joined Mild Steel and Iron's plot at 0.45 s.

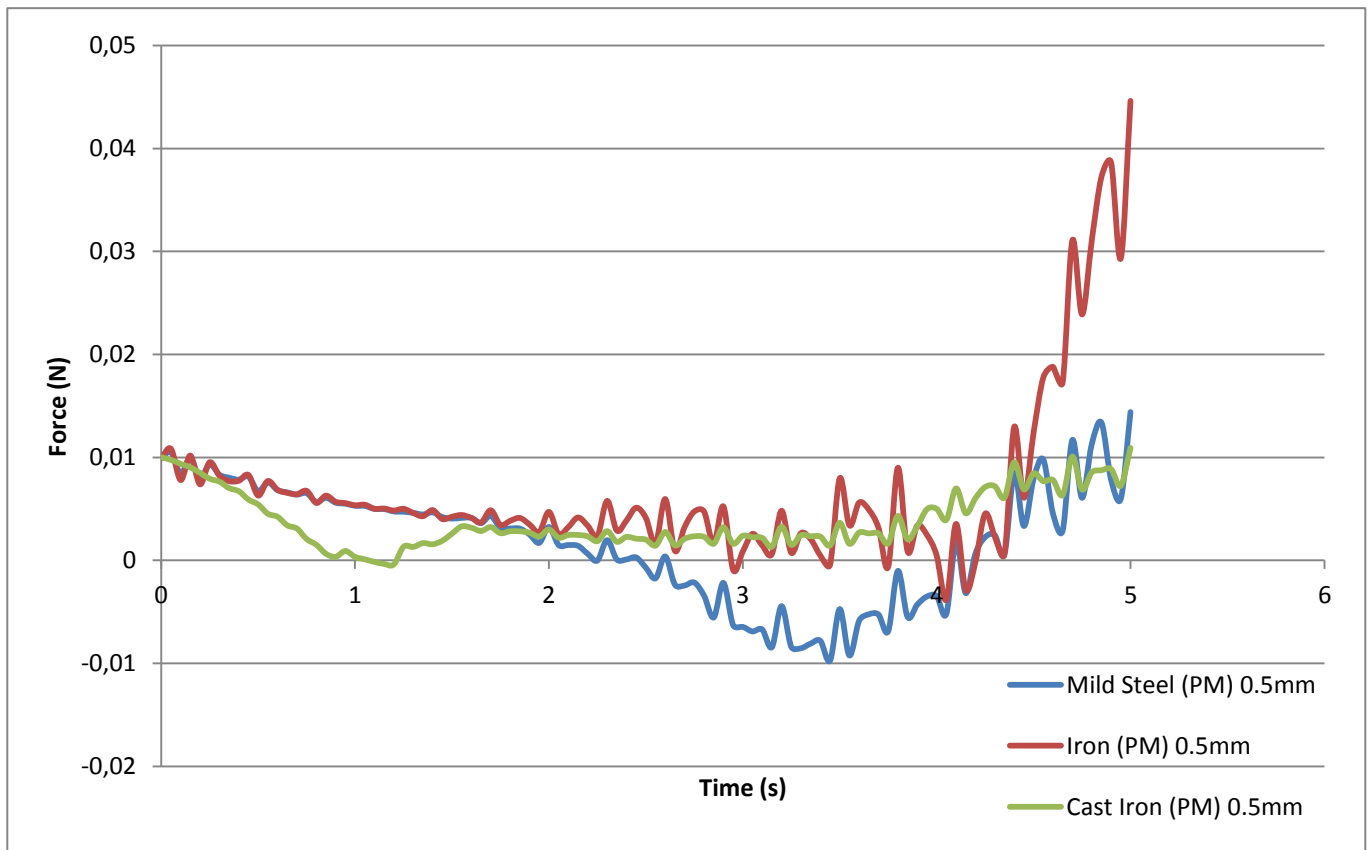
With closer air gaps, alloys coupled with PMs are shown to behave in a same pattern. Therefore, the study of air gap = 0.5mm was extended to 5s to show how they deviated with respect to time.

### 5.4.5 Air Gap of 0.5 mm with extended time (5s)



**Graph 5-9:** Force (N) vs Time (s) without PM; air gap = 0.5mm

**Observation:** With the study extended to 5 s, Mild Steel showed near sinusoidal oscillation with an increase in amplitude at an increasing rate after each successive oscillation. Iron maintained its calm and predictable composure but has a lower magnitude compared to Mild Steel. Cast Iron only showed changes after 3 s with minor amplitudes.



**Graph 5-10:** Force (N) vs Time (s) with PM; air gap = 0.5mm

**Observation:** With the extended study, Mild Steel and Iron deviated away at 1.8 s with Iron becoming relatively unstable towards the end as its equilibrium is shifted upwards in the positive y-direction. Mild Steel remains relatively stable and shifts its equilibrium in the negative and positive y-axis. Cast Iron showed signs of change after 0.8 s and again has small amplitude if compared to the other two alloys with its equilibrium staying slightly above positive y-axis.

## 5.5 Results and Discussions

With respect to Graph 5-1, without the presence of magnet, the force output of iron was the highest followed by Mild Steel and Cast Iron having their equilibrium shifted downwards in the y-axis. A pulse current source was applied and its specifications listed in Table 5-1. According to left hand coil rule, direction of magnetic field is determined by the direction of current flow. By altering the direction of current, the magnetic field can be changed to either attract or repel the thrust disc laminated by a layer of PM. From observation, iron seems to be performing the best with near-sinusoidal pattern. For Mild Steel and Cast Iron, the plots are relatively unstable and could be due to non-linear effects such as built up eddy currents and hysteresis effect opposing the existing current source and causing a magnetic lag as shown in the B-H curve in Chapter 3. Iron with little impurities is best fitted with actuator without a PM.

With the additions of PMs shown in Graph 5-2, Mild Steel showed its sensitivity towards the changing magnetic field by displaying sinusoidal patterns in its plot with the equilibrium shifting downwards and upwards. However, Iron did not show any change to the magnetic field. Although Cast Iron possesses a larger magnitude in the negative y-axis, it only showed minor alternations after 0.4 s. All three alloys yielded significantly larger force output due to the net magnetic flux produced by the PMs and EMs. The force plot started at 0.005 N, which is believed to be caused by the “remanence” effect left by the PM on the actuator as stated in Chapter 3. In hindsight, this thesis is aimed at improving the design of an existing electromagnetic actuator for active vibration control and according to control theory; the sensitivity to change is highly desirable as it awards the user with more control over the system. With Mild Steel coupled with a PM, it showed its sensitivity towards changing magnetic fields and is best suited for actuators that intend to use PM in the design.

With a closer air gap set to 2 mm, Graph 5-3 shows that Iron and Mild Steel maintained similar plots with Iron yielding a higher force magnitude. Cast Iron showed little response to change of magnetic field and had very low force output. When coupled with a PM, all three alloys started their force plot at 0.015 N as shown in Graph 5-4, an increase from the previous air gap of 3 mm. This suggests that the “remanence” effect is significant if there is a presence of a permanent magnet in the actuator. Again, Mild Steel showed its sensitivity towards change with Iron showing the opposite. Cast iron displayed a sudden force surge in the positive y-axis and joined Mild steel’s plot after 0.6 seconds. Cast Iron was seen to be very

unstable and its behaviour unpredictable when coupled with a PM. The study was then done for air gaps of 1 mm and 0.5 mm to investigate the correlation between the actuator's material and its performance.

According to Graph 5-5 with an air gap of 1 mm, Iron showed predictable and near-sinusoidal with respect to time. Mild Steel followed the pattern of Iron but often shows stagnant plots after 0.2 s with its force magnitude being lower than Iron. On the other hand, Cast Iron was sensitive to change but its amplitude being relatively lower if compared to Graph 5-1 with an air gap of 3 mm, emphasizing its unpredictable behaviour. With a closer air gap, Iron showed that its pattern is predictable compared to previous results. Mild Steel was behaving similarly but showed a decrease in amplitude. Concluding from this, steel with more carbon content tends to perform poorly in a changing magnetic field. According to the permeability table in Table 3-2, the permeability of a ferromagnetic metal decreases with increasing carbon content with Iron having a relative permeability of 5000 and mild steel having one of 2000. Relative permeability is directly proportional to force as stated in Equation 3.26. The results shown in Graph 5-1, 5-3, and 5-5 shows that with closer air gaps, the force output of the three alloys are in compliance with the relative permeability table having Iron to be the highest, Mild Steel the second highest and Cast Iron being the lowest.

However, when coupled with a magnet as shown in Graph 5-6, the three alloys were seen to have plots having similar behaviour. Mild Steel was showing slightly higher amplitude than Iron. Although Cast Iron followed the path of Mild Steel and Iron, it did not show any major changes, having linear characteristic and only after 0.5 s, it joined the plot of Mild Steel towards the end. With a closer air gap, the behaviour of the three alloys converged. With a PM, the behaviour of Mild Steel is still very desirable in active vibration control. A final study of 0.5 mm air gap was conducted.

With an air gap of 0.5 mm shown in Graph 5-7, Mild Steel for the first time had higher force amplitude with respect to time compared to iron. Cast Iron again showed that it has the lowest force output. Previous discussion and observation implied that Iron had higher force output based on the permeability table and simulation results. Conversely, Mild Steel was not expected to have a higher force output than Iron. Despite the higher force output, the amplitude of oscillation was increasing at an increasing rate. Iron was having constant amplitude and its behaviour inversed to the ones shown in previous air gaps, possessing an increase in amplitude after every successive period. This demonstrates that the relative

permeability table is not applicable when the air gaps are smaller and that Mild Steel and Iron will show non-linear properties only simulation results can display.

When coupled with a magnet as shown in Graph 5-8, the behaviour of the three alloys further converges with Cast Iron having a peak magnitude at 0.4 s and joining Mild Steel's plot at 0.5 s. This agrees with the results previously with an air gap of 1 mm. However, the behaviour of mild steel and iron cannot be the same since it has different carbon contents. This study was then extended to 5 seconds to show how the alloys deviated away from each other.

Graph 5-9 shows that Mild Steel continues to increase its amplitude after each successive period with Iron maintaining its calm and predictable composure. Cast Iron performed poorly in terms of response and force output, showing signs of change after 3 s. With all the studies simulated, it can be concluded that Iron performed the best without the presence of a magnet since its force plots are relatively stable compared to Mild Steel and Cast Iron.

Graph 5-10 shows that Mild Steel and Iron deviated away at around 1.8 s, with iron becoming increasingly unstable with respect to time. Mild Steel's amplitude appears to be similar and has its equilibrium shifted from the negative to positive y-axis. Cast Iron only started oscillating significantly after 0.8 s and its equilibrium staying in the positive y-axis. Although relatively stable, its insensitivity to change and low force output was discouraging. With respect to all the studies done, Mild Steel proved victorious when coupled with a magnet as it exhibits high sensitivity towards change of magnetic field.

Overall, Mild Steel would be the best coupled with a PM, followed by Iron with Cast Iron out of the question. With Iron containing the least carbon content and cast iron the most, the results show that too much C-content makes the force output of the actuator less susceptible to change. However, having less C-content doesn't mean that the alloy will guarantee the actuator's performance. There is this misconception that higher relative electromagnetic permeability will have higher force output and it is only true for large air gaps. A closer air gap will lead to the misbehaving of predicted and desired responses. With the presence of a magnet, the relative permeability table cannot be used and will need to rely on simulations and testing, with simulation results showing Mild Steel having exceptional results due to its sensitivity to change.

## **5.6 Errors and Restrictions**

During the simulation, the effects of the brass bush were neglected. This might cause discrepancies in the results when real life testing is conducted on the electromagnetic actuator. Brass is an alloy with a combination of copper and zinc, both possessing relative electromagnetic permeability. However, the brass bush was assigned as air during studies to neglect its effect because no suitable material was available to be assigned.

The force magnitudes presented in Graph 5-1 to 5-9 does not agree with the data measured on the old actuator (no PM). The old actuator was made of mild steel which had a maximum force output of 3 N with a minimum air gap of 0.42 mm at current amplitude of 2 Amps based on static testing (Woffenden 2004). For example, Graph 5-9 should have a similar magnitude as well but had a maximum magnitude of 0.00008 N at 5 s instead. This could be due to the short amount of time the studies were subjected during simulation. This can be rectified by calibrating the results obtained from the old actuator and extending the period of studies.

Despite the difference in magnitudes, the studies serve as a good indicator on which material behaves the best when coupled with a PM, a major objective of this thesis.



## **6 Conclusion and Recommendations**

Magnetic bearings have always been used to damp vibration present in a shaft for almost half a century with the first patent emerging in 1944. The working principle of magnetic bearings are based on force exerted by the coils (stator) to stabilize the thrust disc (rotor) connected to the shaft. However, this thesis is aimed at improving the design of an old electromagnetic actuator whose design is derived directly from a magnetic thrust bearing and subsequently meant for active vibration control.

Extensive literature reviews have been conducted to compile past work and research dedicated for magnetic bearings. One of the most suggested ideas is to replace the thrust disc with a permanent magnet (PM) to increase the actuator's force output. The new electromagnetic actuator was designed to be superior to the old one by changing the mechanism that holds the shaft into place, making the coil casings bigger to enable more magnetic flux transfer and dissipation of heat, and finally laminating the thrust disc with ceramic ferrite magnets (PM). The design was drawn in SolidWorks and simulated using an add-in obtained by signing an educational contract with ElectroMagneticWorks. Each part of the actuator was assigned a specific material and studies run on it as the effects of relative permeability on the actuator were non-linear and cannot be numerically calculated. Studies were run with different air gaps to observe the relationship between the alloys and the force output of the coil casings to the thrust disc.

Further simulations concluded that mild steel was the superior alloy as the core metal and thrust disc material compared to iron and cast iron with the presence of a PM. An interesting hypothesis was made where the presence of graphite instead of carbon in the microstructure of a ferromagnetic alloy will make the metal hard to demagnetized and thus not suitable to be paired with time varying current. However, having too little carbon content which increases the relative permeability of the alloy does not guarantee good performance when subjected to time varying current, a misconception many people have because of non-linear characteristics the PM brings. Therefore, a balance has to be achieved. Mild steel having carbon contents in between iron and cast iron proved to be the best when simulations were completed. While coupled with a PM, mild steel is more susceptible to change its magnetic field with respect to time (frequency which the actuator vibrates), a feature not mentioned in books and journals. Ultimately, this characteristic is important in vibration control.

One of the errors encountered during the simulations was the low force the thrust disc was subjected to. This could be caused by wrong settings or undefined parameters in the highly sophisticated simulation software. The amount of time the studies were subjected to was short as well. Although the magnitude of the forces were lower than expected, the amount of studies ran served as an indicator on which alloy performs the best and how they behaved when subjected to time varying current.

The original objectives of this dissertation included in the progress report were achieved wholly by eliminating the external springs, changing the thrust disc to a PM, investigating the effect of permeability and hysteresis effect on the output of the system, and also research on the optimization of the coil design. After the changes made, simulations were conducted and data analysed.

The project could be developed further by testing the electromagnetic actuator via active vibration control and results compared with the old actuator and simulation results. It is crucial to note that mild steel will only produce a higher force output *with* the presence of a PM. Due to time constraints; the actuator was not tested in real life.

Finally, this thesis has highlighted the importance of material selections and how they affect the performance of the actuator. Proper adjustments based on calculations and valid assumptions have been taken into account while designing the new actuator. Nonetheless, real life dynamic testing has to be done to the actuator for the sake of comparing it to the performance of the old one.

[...]